Reconstruction method of local density fluctuation for heavy ion beam probe measurements

H. Nakano, A. Fujisawa, A. Shimizu, S. Ohshima, H. Iguchi, Y. Yoshimura, and T. Minami
National Institute for Fusion Science, Oroshi-cho, Toki 509-5292, Japan

(Received 14 March 2007; accepted 7 May 2007; published online 12 June 2007)

Heavy ion beam probe (HIBP) is an excellent diagnostic to measure the density and potential fluctuations simultaneously in magnetically confined plasmas. However, it has been well known that the density fluctuation measured with the HIBP is not local but contains the fluctuations along the beam orbits. In this article, a method is proposed to evaluate local density fluctuation in the HIBP measurements by removing the well-known path integral effects. The reconstructed density fluctuation amplitude and power spectrum are shown, for example, by applying the proposed method on the density fluctuation measurement data obtained in a toroidal helical plasma, Compact Helical System. © *2007 American Institute of Physics.* [DOI: 10.1063/1.2745233]

I. INTRODUCTION

Precise measurement of turbulence is a key issue for understanding anomalous transport in magnetic confinement plasma since the anomalous transport is caused by fluctuations of density, temperature, and potential. Many diagnostics have been developed to investigate properties of plasma turbulence to understand, and possibly control the transports in a magnetic confinement plasma, such as Langmuir probes, reflectometery, beam emission spectroscopy, electron cyclotron emission spectroscopy, etc.[1]

Heavy ion beam probe[2] (HIBP) is one of the diagnostics used for the turbulence measurements. The advantages of the HIBP are that it can measure simultaneously the density and potential fluctuations even in the interior of high temperature plasmas with high temporal ($\sim\mu$s) and spatial ($\sim$mm) resolutions. Owing to the advantages, the HIBPs have been installed on many of magnetic confinement devices, e.g., Impurity Study Experiment Tokamak-B (ISX-B),[3] Torus Experiment for Technology (-U) (TEXT(-U)),[4] Japanese Institute of Plasma Physics Torus-II Upgrade (JIPPT-IIU),[5] and JAERI Fusion Torus-2 Modified (JFT-2M)[6] in Tokamak; Advanced Toroidal Facility (ATF),[7] Compact Helical System (CHS),[8] and Large Helical Device (LHD)[9] in helical device; and GAMMA-10[10] in mirror device.

It is well known, however, that the density fluctuation measured with the HIBP is not completely local, but is contaminated with the density fluctuation along the beam orbit. Several papers have been published on this path integral effect. These works evaluate how the path integral fluctuation affects the measurement of a wave number spectrum,[11,12] and how the measured fluctuation amplitude is different from the real local density fluctuation amplitude.[13] In contrast to these works, a preliminary method was proposed to infer the real local density fluctuation amplitude from the measured one.[14] The present article proposes an extended method to reconstruct the local density fluctuation in the HIBP measurements, and provides the obtained results of the local density fluctuation using the proposed method applied on density fluctuation data in CHS.

II. RECONSTRUCTION METHOD OF LOCAL DENSITY FLUCTUATION

A. Brief description of density fluctuation measurements of HIBP

The HIBP system consists of an accelerator, an energy analyzer, and beam sweepers. In principle, a singly charged heavy ion beam, termed primary beam, is injected into a plasma. In the plasma, the beam ions are ionized to doubly (or higher) charged ions through the collisions with plasma particles, usually electrons. The doubly charged ions, called a secondary beam, come out from the plasma, and are detected with the energy analyzer.

The detected beam current I_d is expressed in the following form:

$$I_d(r_*) = 2I_0 l_{\mathrm{sv}} n_e(r_*) \frac{\langle \sigma_{12} v_e \rangle_M}{v_b} \exp\left(- \int_{l_1} \frac{n_e(r_1)\langle \sigma_1 v_e \rangle_M}{v_b} dl_1 - \int_{l_2} \frac{n_e(r_2)\langle \sigma_2 v_e \rangle_M}{v_b} dl_2 \right), \quad (1)$$

where r_* is an ionization position, I_0 is the initial primary beam current, l_{sv} is the sample volume length, v_e is the electron thermal velocity, v_b is the beam velocity, n_e is the electron density, σ_{12} is the electron impact ionization cross section from singly charged ion to doubly charged ion at the sample volume, σ_i $(i=1,2)$ is the cross section from i-charged ion to higher charged ion, and dl_1 and dl_2 are the infinitesimal length elements of primary and secondary orbits, respectively. A bracket $\langle\ \rangle_M$ means the average with the Maxwellian velocity distribution. Hence, the detected beam current is dependent on the electron density at the ionization point and the attenuation along the beam orbit. According to the expression, the detected beam current is proportional to the local density and attenuation along the primary and secondary beam orbits.

By taking variations of Eq. (1), the detected beam current fluctuation is described in a normalized form,

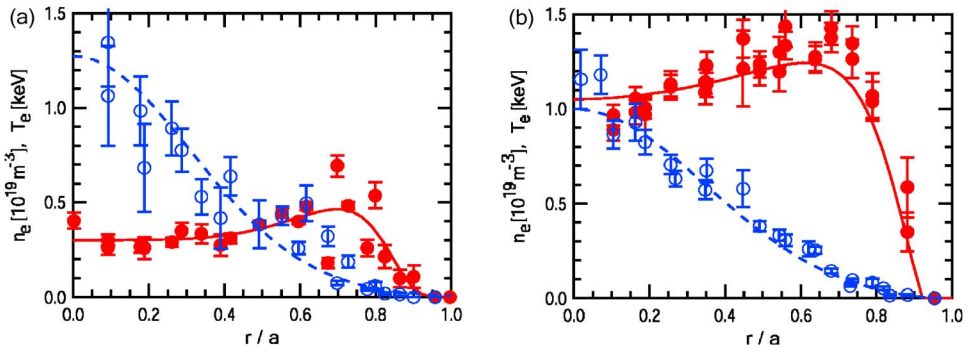

FIG. 1. Profiles of electron density (filled circles) and temperature (open circles) for the density fluctuation measurements using HIBPs in CHS. (a) Those in the ECR-heated plasma with the line averaged density of $\bar{n}_e = 4.7 \times 10^{18}$ m^{-3} (low density plasma), and (b) those of $\bar{n}_e = 9.5 \times 10^{18}$ m^{-3} (high density plasma).

$$\tilde{\eta}(\rho_*) = \tilde{\xi}(\rho_*) - \int_{l_1} \tilde{\xi}(\rho_1) S_1(\rho_1) w_1(\rho_1) d\rho_1 - \int_{l_2} \tilde{\xi}(\rho_2) S_2(\rho_2) w_2(\rho_2) d\rho_2, \quad (2)$$

where $\rho \equiv r/a$ is the normalized minor radius, $S_i(\rho) \equiv (n_e(\rho)\langle \sigma_i v_e(\rho)\rangle_M a)/v_B$ is the normalized ionization rate, $\tilde{\eta}(\rho) \equiv (I_d(\rho) - \langle I_d(\rho)\rangle_E)/\langle I_d(\rho)\rangle_E$ is the normalized fluctuations of the detected beam current, and $\tilde{\xi}(\rho) \equiv (n_e(\rho) - \langle n_e(\rho)\rangle_E)/\langle n_e(\rho)\rangle_E$ is the normalized fluctuations of the local density. The ionization rate $S_i(\rho)$ is a function of the density, temperature, and beam velocity. The ionization rates are derived from atomic and molecular database or empirical formulas. The integral variable is converted from the path length to the normalized radius by introducing $w_i(\rho_i) \equiv \partial l_i(\rho_i)/\partial \rho_i$. In deriving Eq. (2), two assumptions are made: (i) the temperature fluctuation leading to the fluctuation of ionization rate is neglected, and (ii) the density fluctuation is homogeneous on the same flux surface, although poloidal asymmetry in density fluctuation has been found in some experiments.[15]

B. Derivation of integral equation of local density fluctuation

By taking ensemble averages of Eq. (3), the fluctuation power of the detected beam current is expressed as

$$\begin{aligned}\langle \tilde{\eta}^2(\rho_*)\rangle_E = {} & \langle \tilde{\xi}^2(\rho_*)\rangle_E - 2\int_{l_1} \langle \tilde{\xi}(\rho_*)\tilde{\xi}(\rho_1)\rangle_E S_1(\rho_1) w_1(\rho_1) d\rho_1 - 2\int_{l_2} \langle \tilde{\xi}(\rho_*)\tilde{\xi}(\rho_2)\rangle_E S_2(\rho_2) w_2(\rho_2) d\rho_2 \\ & + \int\int_{l_1 l_1'} \langle \tilde{\xi}(\rho_1)\tilde{\xi}(\rho_1')\rangle_E S_1(\rho_1) S_1(\rho_1') w_1(\rho_1) w_1(\rho_1') d\rho_1 d\rho_1' \\ & + \int\int_{l_2 l_2'} \langle \tilde{\xi}(\rho_2)\tilde{\xi}(\rho_2')\rangle_E S_2(\rho_2) S_2(\rho_2') w_2(\rho_2) w_2(\rho_2') d\rho_2 d\rho_2' \\ & + 2\int\int_{l_1 l_2} \langle \tilde{\xi}(\rho_1)\tilde{\xi}(\rho_2)\rangle_E S_1(\rho_1) S_2(\rho_2) w_1(\rho_1) w_2(\rho_2) d\rho_1 d\rho_2, \end{aligned} \quad (3)$$

where a bracket $\langle\ \rangle_E$ denotes the ensemble average. The second and third terms represent the first order path integral effect, while the other integral terms from the fourth to sixth do the second order path integral effect. The physical meanings of these two kinds of path integral effects are explained in Appendix A. The correlation terms $\langle \tilde{\xi}(\rho_i)\tilde{\xi}(\rho_j)\rangle_E$ can be expressed as

$$\langle \tilde{\xi}(\rho_i)\tilde{\xi}(\rho_j)\rangle_E = \langle |\tilde{\xi}(\rho_i)|\rangle_E \langle |\tilde{\xi}(\rho_j)|\rangle_E \Gamma(\rho_i, \rho_j) \quad (i = 1,2, j = 1,2) \quad (4)$$

using the correlation function $\Gamma(\rho_i, \rho_j)$. Then the measured density fluctuation with the path integral terms, as is shown in Eq. (3), is represented by the integral equation for the local density fluctuations. The local density fluctuation can be obtained as a solution of the integral equation if the correlation function is known. In other words, the integral equation can be solved if the two-point correlation property of local density fluctuations $\Gamma(\rho_i, \rho_j)$, and the density and temperature profiles are known.

C. Extention of integral equation to Fourier components

The integral equation, Eq. (3), is easily extended to the relationship between the Fourier components of local fluctuation and the one with path integral effect, as

$$\langle|\tilde{\eta}_F(\rho_*)|^2\rangle_E = \langle|\tilde{\xi}_F(\rho_*)|^2\rangle_E - 2\int_{l_1}\langle\tilde{\xi}_F^*(\rho_*)\tilde{\xi}_F(\rho_1)\rangle_E S_1(\rho_1)w_1(\rho_1)d\rho_1 - 2\int_{l_2}\langle\tilde{\xi}_F^*(\rho_*)\tilde{\xi}_F(\rho_2)\rangle_E S_2(\rho_2)w_2(\rho_2)d\rho_2$$
$$+\int\int_{l_1l_1'}\langle\tilde{\xi}_F^*(\rho_1)\tilde{\xi}_F(\rho_1')\rangle_E S_1(\rho_1)S_1(\rho_1')w_1(\rho_1)w_1(\rho_1')d\rho_1 d\rho_1'$$
$$+\int\int_{l_2l_2'}\langle\tilde{\xi}_F^*(\rho_2)\tilde{\xi}_F(\rho_2')\rangle_E S_2(\rho_2)S_2(\rho_2')w_2(\rho_2)w_2(\rho_2')d\rho_2 d\rho_2'$$
$$+\int\int_{l_1l_2}\langle\tilde{\xi}_F^*(\rho_1)\tilde{\xi}_F(\rho_2)\rangle_E S_1(\rho_1)S_2(\rho_2)w_1(\rho_1)w_1(\rho_2)d\rho_1 d\rho_2, \quad (5)$$

where subscript F means Fourier component of fluctuation, and the correlation terms can be expressed, in a similar way to Eq. (4), as

$$\langle\tilde{\xi}_F^*(\rho_i)\tilde{\xi}_F(\rho_j)\rangle_E = \langle|\tilde{\xi}_F(\rho_i)|\rangle_E\langle|\tilde{\xi}_F(\rho_j)|\rangle_E\gamma_F(\rho_i,\rho_j) \times\cos[\varphi_F(\rho_i,\rho_j)], \quad (6)$$

where $\gamma_F(\rho_i,\rho_j)$ and $\varphi_F(\rho_i,\rho_j)$ are the coherence and phase difference between $\tilde{\xi}_F(\rho_i)$ and $\tilde{\xi}_F(\rho_j)$ at the frequency ω, respectively. Therefore, the power spectrum of the local density fluctuation can be obtained by solving Eq. (5) for $\tilde{\xi}_F(\rho)$.

III. EXAMPLES OF THE RECONSTRUCTION USING EXPERIMENTAL DATA

A. Application of proposed method on CHS data

CHS,[16] which generates a toroidal plasma with the major and minor radii being 1.0 and 0.2 m, has two HIBPs installed. Here, we have applied the proposed reconstruction method on the data of the HIBP density fluctuation measurements in electron cyclotron resonance (ECR)-heated discharges of two different density regimes, $\bar{n}_e = 4.7\times10^{18}$ m^{-3} (low density) and $\bar{n}_e = 9.5\times10^{18}$ m^{-3} (high density). The measurements were performed on the discharges. In the measurement, the cesium beam of ~70 keV is used for the experiments with magnetic field strength of 0.9 T.

In order to solve the integral equation, Eq. (3), it is necessary to evaluate the ionization rate and correlation function $\Gamma(\rho_i,\rho_j)$. The ionization rate is estimated using Lotz's empirical formula[17] since the density and temperature profiles are known from a multipoint Thomson scattering system, as is shown in Fig. 1. In contrast, although the correlation function $\Gamma(\rho_i,\rho_j)$ is rather difficult to estimate since it requires a wide range of the fluctuation measurement over a whole plasma region, we assume here that the correlation function $\Gamma(\rho_i,\rho_j)$ should be described as $\Gamma(\rho_i,\rho_j)\equiv\exp[-(\rho_i-\rho_j)^2/2l_{\text{global}}^2(\rho_i,\rho_j)]$, where $l_{\text{global}}(\rho)$ signifies the normalized correlation length. Under this assumption, the problem to obtain the correlation function can be ascribed to determining the correlation length.

The HIBP on CHS has three channels to observe the fluctuations at the adjacent points in the plasma simultaneously. The neighboring observation points are located ~1 cm apart from each other according to a trajectory calculation. From the correlation between these neighboring two channels, the normalized local correlation length can be estimated in the following way, $\Gamma(\rho,\rho+\delta\rho)=\langle\tilde{\xi}(\rho)\tilde{\xi}(\rho+\delta\rho)\rangle_E/\langle|\tilde{\xi}(\rho)|\rangle_E\langle|\tilde{\xi}(\rho+\delta\rho)|\rangle_E=\exp[-\delta\rho^2/2l_{\text{local}}^2(\rho)]$. By taking the symmetric characteristic into consideration, the global correlation length can be possibly assumed as $1/l_{\text{global}}(\rho_i,\rho_j)=[1/l_{\text{local}}(\rho_i)+1/l_{\text{local}}(\rho_j)]/2$. In this expression, the global correlation length $l_{\text{global}}(\rho_i,\rho_j)$ becomes closer to $l_{\text{local}}(\rho_i)$ when $\rho_j\to\rho_i$.

Figure 2 shows the evaluation of the local correlation length using this approximation as a function of normalized radius. Here, the measured density fluctuation is used instead of the local density fluctuation for the estimation of the local correlation length practically. In other words, the local correlation length is estimated in the zeroth order approximation, from $\Gamma(\rho,\rho+\delta\rho)=\exp[-\delta\rho^2/2l_{\text{local}}^2(\rho)]\simeq\langle\tilde{\eta}(\rho)\tilde{\eta}(\rho+\delta\rho)\rangle_E/\langle|\tilde{\eta}(\rho)|\rangle_E\langle|\tilde{\eta}(\rho+\delta\rho)|\rangle_E$. The result shows that the correlation length increases toward the edge, which is 5 mm in the center and more than 15 mm near a last closed flux surface. In addition, the local correlation length in high density plasma tends to be slightly longer than that in low density.

The results of the reconstructed local density fluctuation are shown in Fig. 3 for the two density regimes. The open

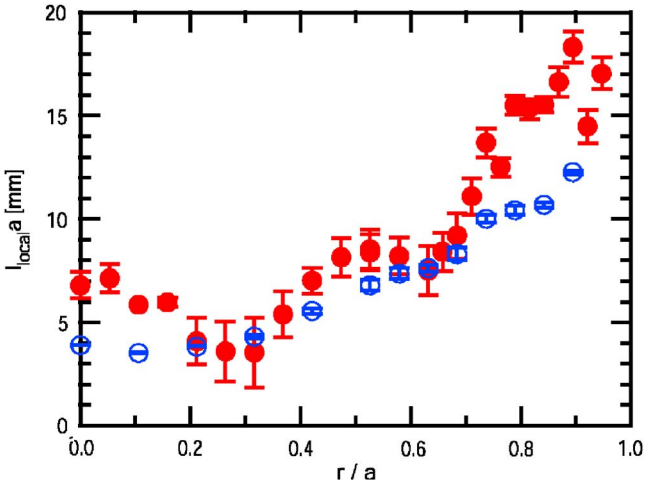

FIG. 2. The local correlation lengths in the zeroth order approximation as a function of normalized minor radius. The open and filled circles represent the correlation lengths in the low ($\bar{n}_e = 4.7\times10^{18}$ m^{-3}) and high density plasmas ($\bar{n}_e = 9.5\times10^{18}$ m^{-3}) in Fig. 1, respectively.

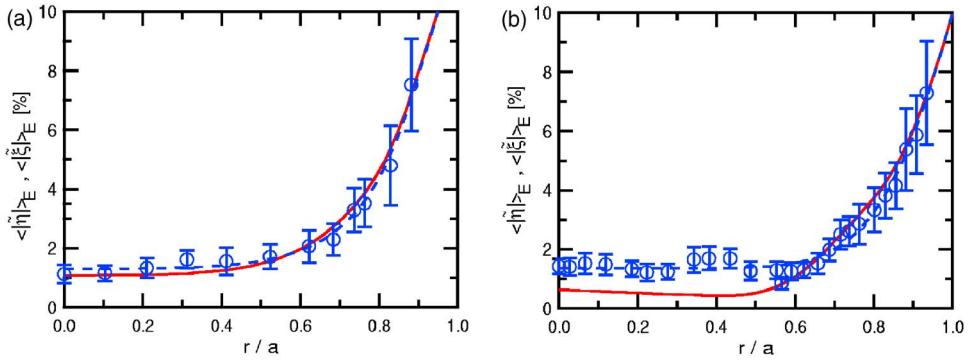

FIG. 3. The profiles of measured and reconstructed density fluctuation amplitudes in the cases of (a) the low and (b) high density plasmas in Fig. 1. The open circles (fitted with the dashed lines) and the solid lines represent the measured fluctuation and the reconstructed density fluctuation amplitudes, respectively.

circles represent the amplitude of the measured density fluctuation containing the path integral effect $\langle|\tilde{\eta}|\rangle_E$. The solid line shows the reconstructed local density fluctuation, while the dashed line is a fitting curve for the experimental data. In the lower density case, the profile of local density fluctuation amplitude $\langle|\tilde{\xi}|\rangle_E$ is everywhere within the range of statistical error bars [Fig. 3(a)]. In contrast, the amplitude of the local density fluctuation is significantly smaller than that of the measured density fluctuation [Fig. 3(b)] in $\rho<0.6$, although no significant difference of amplitude between the local density fluctuation and the measured density fluctuation in $\rho>0.6$ can be seen for the case of high density plasma. Here, the amplitude of the measured density fluctuation reaches up to 1.5 times larger than that of the local density fluctuation owing to the path integral effect.

B. Reconstruction of power spectrum

The reconstruction of local power spectrum of density fluctuation can be performed as a straightforward extension of that of the local fluctuation amplitude in the previous subsection. The reconstruction of power spectrum can be performed using Eq. (5) by estimating the correlation length for each frequency from coherence $\gamma_F(\rho_i,\rho_j)$, with assuming the phase $\cos[\varphi_F(\rho_i,\rho_j)]\equiv 1$. As is similar to the previous procedure,

$$\gamma_F(\rho_i,\rho_j)=\exp[-(\rho_i-\rho_j)^2/2l^2_{\mathrm{global},F}], \tag{7}$$

where $1/l_{\mathrm{global},F}=[1/l_{\mathrm{local},F}(\rho_i)+1/l_{\mathrm{local},F}(\rho_j)]/2$, where $l_{\mathrm{global},F}$ and $l_{\mathrm{local},F}$ are Fourier components of global and local correlation lengths, respectively.

For the previous reconstruction of the local density fluctuation amplitude, the zeroth order approximation of the correlation length is sufficient to obtain a significant solution of Eq. (3). However, for the reconstruction of the power spectrum, particularly for a lower frequency range, first order correction of the correlation length is necessary (see Appendix B). The zeroth order estimation, $\gamma_F(\rho_i,\rho_j)\sim\langle\tilde{\eta}_F(\rho_i)\eta_F(\rho_j)\rangle_E/\langle|\tilde{\eta}_F(\rho_i)|\rangle_E\langle|\tilde{\eta}_F(\rho_j)|\rangle_E$, gives a falsely long correlation length, due to the path integral effect on the correlation length, so that a negative power density is often obtained. Figure 4 shows the difference between the zeroth order correlation length and one with the first order correction in the low density plasma. The difference of correlation lengths between before and after the correction tends to be larger in low frequency. The corrected correlation length becomes shorter in smaller radii ($\rho<0.6$), while the length slightly longer in large radii ($\rho<0.6$), as is similar to the amplitude reconstruction of the local density fluctuation.

Figure 5 shows the measured and the reconstructed power spectra of the local density fluctuation at $\rho=0.23$ and $\rho=0.73$ in the low and high density plasmas. Here we define a parameter to indicate the degree of distortion, as $D_{\mathrm{ist},F}\equiv(\langle|\tilde{\eta}(\rho)|\rangle_E-\langle|\tilde{\xi}(\rho)|\rangle_E)/\langle|\tilde{\xi}(\rho)|\rangle_E$. In the low density case, the difference between the measured and reconstructed power spectra is not significant except the region of less than $\sim$15 kHz at $\rho=0.23$. It should be notified that the power spectrum of the measured density fluctuation is smaller than that of the local density fluctuation (i.e., $D_{\mathrm{ist},F}\sim-10\%$) in less than 15 kHz at $\rho=0.73$ due to the first order path integral effect or the screening effect (see Appendix A). On the other hand, in the high density case, the power spectrum is strongly distorted due to the path integral effect; $D_{\mathrm{ist},F}$ can reach up to 55% at $\rho=0.23$. All examples show that the path integral effect becomes small with high frequency owing to the shorter correlation length.

IV. DISCUSSION

Here, we propose a method to reconstruct the local density fluctuation from the one with the path integral effects. In

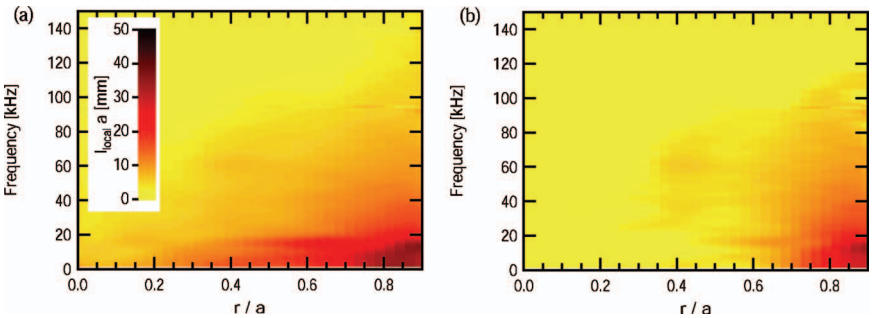

FIG. 4. (Color) The correlation lengths as a function of normalized radius and frequency (a) before and (b) after the correction in the low density plasma.

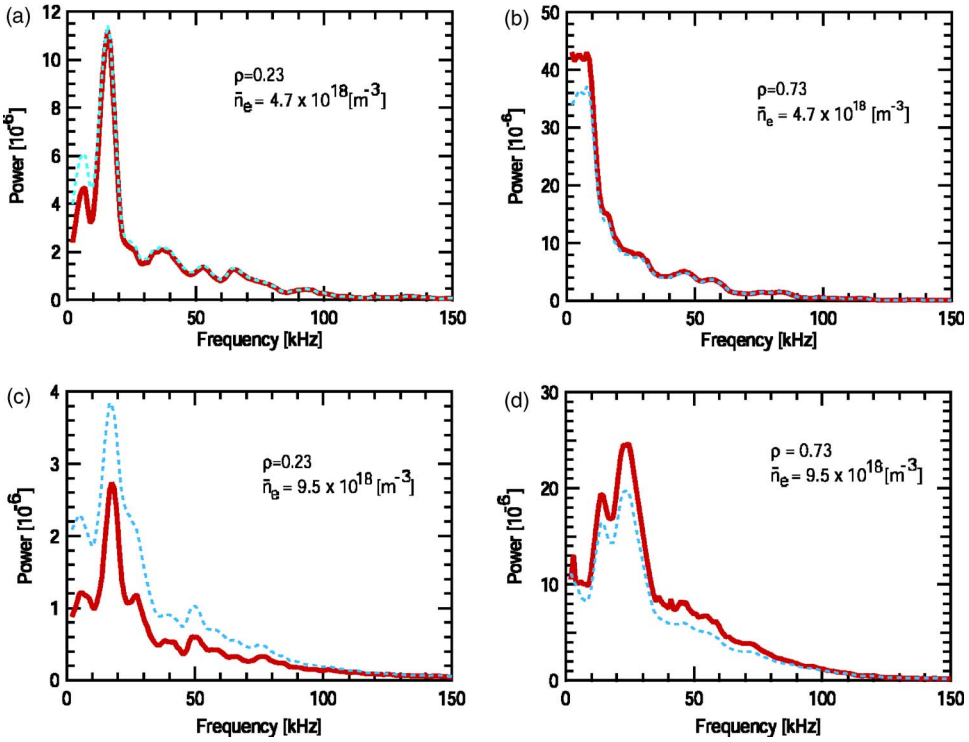

FIG. 5. The power spectra of density fluctuations before and after the reconstruction. The dotted and solid lines are the measured and the reconstructed spectra, respectively. (a) The power spectra at ρ=0.23 and (b) ρ=0.73 in the low density plasma. (c) The power spectra at ρ=0.23 and (d) ρ=0.73 in the high density plasma.

this method, the local density fluctuation can be reconstructed if the spatial characteristics of fluctuations and the ionization cross sections are given. In the presented examples, spatial characteristics of fluctuations can be described by a single parameter, that is, the correlation length.

In this article, quite simple assumptions are adopted for the Gaussian form of the correlation length, which always gives a positive value. Similarly in the treatment of frequency domain, the simplest phase relation $\cos[\varphi_F(\rho_i,\rho_j)] \equiv 1$ is also assumed. These assumptions should maximize the path integral effect. Actually, in the case of the fluctuations driven by magnetohydrodynamics (MHD) modes, the phase information should give a large impact on the evaluation of local density fluctuation amplitude. In this case, the phase information or mode structure can be evaluated from magnetic field measurements. In contrast, in the case of the fluctuation or turbulence driven by the microinstabilities, the correlation length should be short, compared to the minor radius, not to give the serious impact on the reconstruction results. In the presented examples, no sign of MHD instabilities are found in such a low density ECR-heated plasma.

On the other hand, the reconstructed amplitude of local density fluctuation could be sensitive to the correlation length estimation. In order to investigate the sensitivity, we have calculated the local amplitude of density fluctuation using the longest and shortest correlation lengths within the error bars in Fig. 2 in the high density plasma in Fig. 1. The results in Fig. 6 demonstrate that approximately 20% difference is caused by choosing the longest and shortest correlation lengths within the error bars. The precise estimation of the correlation length is one of the important aspects of the reconstruction of the local density fluctuation amplitude.

In the present examples, the ionization cross sections are assumed to obey Lotz's empirical formula. However, it has been known that the formula gives a rather low ionization cross section in larger atoms. Moreover, at present it is difficult to find the precise experimental data of the ionization cross section for the heavier ions, such as cesium, rubidium, thallium, and so on, which are usually used for HIBP measurements. Therefore, the precise estimation of the ionization cross section is another important factor for precise evaluation of the local density fluctuation amplitude. The present method shown in this article is in principle useful and correct in inferring the local density fluctuation; however, there are several uncertainties in essential quantities in order to give accurate evaluation. Finally, the reconstruction method can

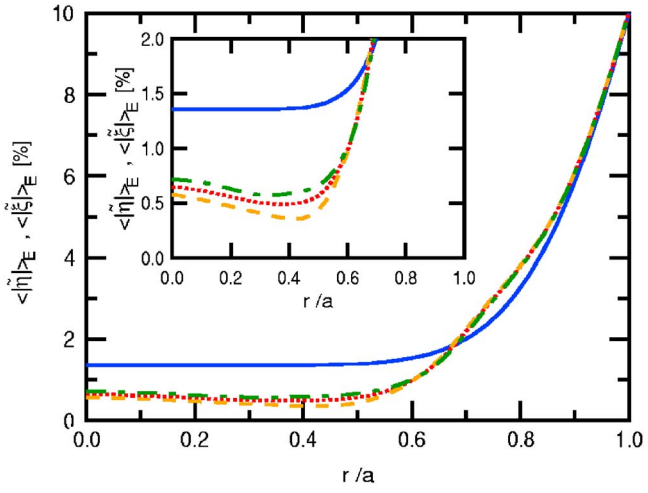

FIG. 6. Uncertainty of the reconstructed density fluctuation amplitude due to the estimation of correlation length. The dotted, dashed, and dashed-dotted lines show the reconstructed density fluctuation amplitudes in the high density plasma using the average, the shortest, and the longest correlation lengths within the error bars of the filled circles in Fig. 2.

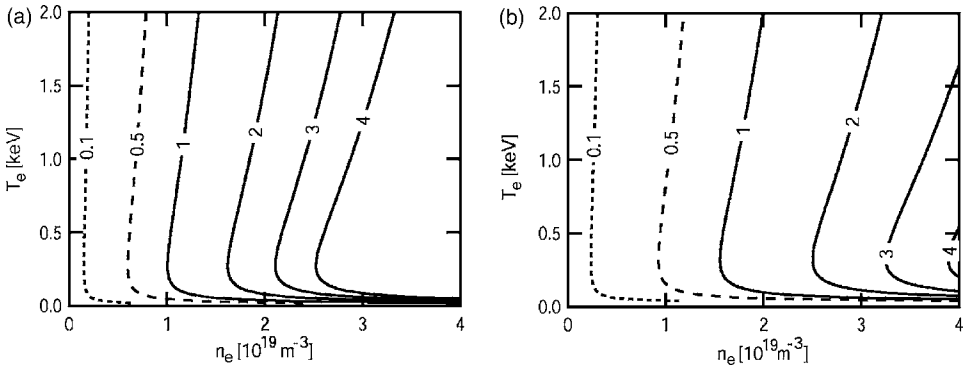

FIG. 7. The evaluated path integral coefficients as a function of the density n_e and temperature T_e in cases of (a) cesium and (b) rubidium beams in CHS.

be applied to other beam probe diagnostics, e.g., lithium beam probe and beam emission spectroscopy.

APPENDIX A: DETAILS OF PATH INTEGRAL EFFECT

In order to understand the physical meaning of the path integral terms in Eq. (3), the correlation of the fluctuations is assumed to obey the form of δ function as

$$\langle\tilde{\xi}(\rho_a)\tilde{\xi}(\rho_b)\rangle_E \equiv \sqrt{2\pi}\langle|\tilde{\xi}(\rho_a)|\rangle_E\langle|\tilde{\xi}(\rho_b)|\rangle_E l_c(\rho_a)\delta(\rho_a - \rho_b)\delta(l_i,l_j), \tag{A1}$$

where l_c is the normalized correlation length. $\delta(l_i,l_j)$ is the Kronecker delta, which is introduced for the assumption that no correlation exists between the fluctuations on primary and secondary orbits. Using the assumed correlation function, Eq. (3) is reduced to

$$\langle\tilde{\eta}^2(\rho_*)\rangle_E = [1 - S_c(\rho_*)]\langle\tilde{\xi}^2(\rho_*)\rangle_E + A_c(l_1,l_2), \tag{A2}$$

where

$$S_c(\rho_*) \equiv 2\sqrt{2\pi}l_c(\rho_*)[S_1(\rho_*) + S_2(\rho_*)], \tag{A3}$$

$$A_c(l_1,l_2) \equiv \sqrt{2\pi}\int_{l_1}\langle\tilde{\xi}^2(\rho_1)\rangle_E l_c(\rho_1)S_1^2(\rho_1)w_1(\rho_1)d\rho_1 + \sqrt{2\pi}\int_{l_2}\langle\tilde{\xi}^2(\rho_2)\rangle_E l_c(\rho_2)S_2^2(\rho_2)w_2(\rho_2)d\rho_2. \tag{A4}$$

The term $A_c(l_1,l_2)$ is derived from the fourth, fifth, and sixth terms in the right-hand side of Eq. (3), and expresses the integrated fluctuations along the beam orbits. Therefore, this term is called accumulation effect. On the other hand, the term $S_c(\rho_*)$ is called screening effect. If the density fluctuation nearby the observation point is positively correlated with the fluctuation at the observation point, the attenuation of the beam due to the neighboring fluctuation gives an out-of-phase contribution to the measured fluctuation, and works as the screening of the local density fluctuation.

Further reduction of Eq. (A1) is possible under the assumption that plasma and density fluctuations are homogeneous. The reduced form of Eq. (A1) is expressed in the following form:

$$\overline{\tilde{\eta}^2} = (1 - \bar{S}_c + \bar{A}_c)\overline{\tilde{\xi}^2}, \tag{A5}$$

$$\bar{S}_c \equiv 2\sqrt{2\pi}l_c(\bar{S}_1 + \bar{S}_2), \tag{A6}$$

$$\bar{A}_c \equiv \sqrt{2\pi}l_c(\bar{S}_1^2 L_1 + \bar{S}_2^2 L_2), \tag{A7}$$

where the overline represents constant in the plasma, and L_1 and L_2 represent the primary and secondary beam orbit lengths normalized by minor radii, respectively.

Here, we can define a path integral coefficient $\bar{\zeta}$ to roughly indicate the degree of the path integral effects,

$$\bar{\zeta} \equiv \bar{S}_c + \bar{A}_c. \tag{A8}$$

Figure 7 shows the dependencies of the path integral coefficients on electron temperature and density for the cases using cesium and rubidium beams in CHS geometry. In the calculation, it is assumed that $l_c=0.05$, $L_1=L_2=1$, and that the beam energies of cesium and rubidium are 70 and 111 keV, respectively. Both the path integral coefficient of cesium $\bar{\zeta}_{\mathrm{Cs}}$ and that of $\bar{\zeta}_{\mathrm{Rb}}$ are dependent strongly on electron temperature in the low temperature range of less than 50 eV. However, in the higher temperature regime, the coefficients, independently of temperature, are almost determined with the density. In comparison, the critical density where the path integral effect becomes significant is higher in rubidium than that in cesium; the density value at which $\bar{\zeta}_{\mathrm{Rb}}=1$ is $n_e=1.7\times10^{19}$ m^{-3}, while the density value at which $\bar{\zeta}_{\mathrm{Cs}}=1$ is $n_e=1.1\times10^{19}$ m^{-3}.

APPENDIX B: PATH INTEGRAL EFFECT ON CORRELATION LENGTH

The correlation length should also suffer from the path integral effect. If there is sufficiently large fluctuation at the edge, the inside fluctuations should contain the edge fluctuation. Therefore, the correlation length appears to be longer than the pure correlation length due to the contamination of the edge fluctuations. Particularly, the effect should be large-for the low frequency fluctuations whose wavelength is expected to be longer. The distortion of the correlation length can be evaluated as follows.

The Fourier components of the measured density fluctuation at two locations ρ_a and ρ_b are represented by

$$\tilde{\eta}_F(\rho_a) = \tilde{\xi}_F(\rho_a) - \int_{l_{a1}}\tilde{\xi}_F(\rho_{a1})S_1(\rho_{a1})w_1(\rho_{a1})d\rho_{a1} - \int_{l_{a2}}\tilde{\xi}_F(\rho_{a2})S_2(\rho_{a2})w_2(\rho_{a2})d\rho_{a2}, \tag{B1}$$

$$\tilde{\eta}_F(\rho_b) = \tilde{\xi}_F(\rho_b) - \int_{l_{b1}} \tilde{\xi}_F(\rho_{b1}) S_1(\rho_{b1}) w_1(\rho_{b1}) d\rho_{b1} - \int_{l_{b2}} \tilde{\xi}_F(\rho_{b2}) S_2(\rho_{b2}) w_2(\rho_{b2}) d\rho_{b2}. \tag{B2}$$

Therefore, the cross correlation of the measured density fluctuation is expressed as

$$\langle \tilde{\eta}_F^*(\rho_a) \tilde{\eta}_F(\rho_b) \rangle_E = \langle \tilde{\xi}_F^*(\rho_a) \tilde{\xi}_F(\rho_b) \rangle_E + \beta_F[\tilde{\xi}_F(\rho_a), \tilde{\xi}_F(\rho_b)], \tag{B3}$$

where $\beta_F[\tilde{\xi}_F(\rho_a), \tilde{\xi}_F(\rho_b)]$ is the path integral term described as

$$\begin{aligned}
\beta_F[\tilde{\xi}_F(\rho_a), \tilde{\xi}_F(\rho_b)] = & - \int_{l_{b1}} \langle \tilde{\xi}_F^*(\rho_a) \tilde{\xi}_F(\rho_{b1}) \rangle_E S_1(\rho_{b1}) w_{b1}(\rho_{b1}) d\rho_{b1} - \int_{l_{b2}} \langle \tilde{\xi}_F^*(\rho_a) \tilde{\xi}_F(\rho_{b2}) \rangle_E S_2(\rho_{b2}) w_{b2}(\rho_{b2}) d\rho_{b2} \\
& - \int_{l_{a1}} \langle \tilde{\xi}_F^*(\rho_b) \tilde{\xi}_F(\rho_{a1}) \rangle_E S_1(\rho_{a1}) w_{a1}(\rho_{a1}) d\rho_{a1} - \int_{l_{a2}} \langle \tilde{\xi}_F^*(\rho_b) \tilde{\xi}_F(\rho_{a2}) \rangle_E S_2(\rho_{a2}) w_{a2}(\rho_{a2}) d\rho_{a2} \\
& + \int \int_{l_{a1} l_{b1}} \langle \tilde{\xi}_F^*(\rho_{a1}) \tilde{\xi}_F(\rho_{b1}) \rangle_E S_1(\rho_{a1}) S_1(\rho_{b1}) w_{a1}(\rho_{a1}) w_{b1}(\rho_{b1}) d\rho_{a1} d\rho_{b1} \\
& + \int \int_{l_{a2} l_{b2}} \langle \tilde{\xi}_F^*(\rho_{a2}) \tilde{\xi}_F(\rho_{b2}) \rangle_E S_2(\rho_{a2}) S_2(\rho_{b2}) w_{a2}(\rho_{a2}) w_{b2}(\rho_{b2}) d\rho_{a2} d\rho_{b2} \\
& + \int \int_{l_{a1} l_{b2}} \langle \tilde{\xi}_F^*(\rho_{a1}) \tilde{\xi}_F(\rho_{b2}) \rangle_E S_1(\rho_{a1}) S_2(\rho_{b2}) w_{a1}(\rho_{a1}) w_{b2}(\rho_{b2}) d\rho_{a1} d\rho_{b2} \\
& + \int \int_{l_{a2} l_{b1}} \langle \tilde{\xi}_F^*(\rho_{a2}) \tilde{\xi}_F(\rho_{b1}) \rangle_E S_2(\rho_{a2}) S_1(\rho_{b1}) w_{a2}(\rho_{a2}) w_{b1}(\rho_{b1}) d\rho_{a2} d\rho_{b1}.
\end{aligned} \tag{B4}$$

The relationship of Fourier components between the cross correlation and the local correlation function is expressed as

$$\gamma_F(\rho_a, \rho_b) \equiv \exp\left(- \frac{(\rho_a - \rho_b)^2}{2 l_{\text{local}}^2(\rho_a, \rho_b)} \right) = \frac{\langle \tilde{\eta}_F^*(\rho_a) \tilde{\eta}_F(\rho_b) \rangle_E - \beta[\tilde{\xi}_F(\rho_a), \tilde{\xi}_F(\rho_b)]}{\langle |\tilde{\xi}_F(\rho_a)| \rangle_E \langle |\tilde{\xi}_F(\rho_b)| \rangle_E}. \tag{B5}$$

The expression shows that the first order correction of the local correlation length can be made by evaluating the path integral term $\beta_F[\tilde{\xi}_F(\rho_a), \tilde{\xi}_F(\rho_b)]$ using the measured density fluctuation instead of the local density fluctuation. The first order correction was essential to reconstruct the local density fluctuation spectrum shown in Fig. 4. Further correction may be possible if the corrected local density fluctuation is substituted into Eq. ((B5))

[1] N. Bretz, Rev. Sci. Instrum. **68**, 2927 (1998).
[2] T. P. Crowley, IEEE Trans. Plasma Sci. **22**, 310 (1994).
[3] G. A. Hallock, A. J. Wootton, and R. L. Hickok, Phys. Rev. Lett. **59**, 1301 (1987).
[4] V. J. Simic *et al.*, Phys. Fluids B **5**, 1576 (1993).
[5] Y. Hamada, A. Nishizawa, Y. Kawasumi, A. Fujisawa, and H. Iguchi, Fusion Eng. Des. **34–35**, 663 (1997).
[6] T. Ido, Y. Hamada, A. Nishizawa, Y. Kawasumi, Y. Miura, and K. Kamiya, Rev. Sci. Instrum. **70**, 955 (1999).
[7] J. J. Zielinski *et al.*, Rev. Sci. Instrum. **61**, 2961 (1990).
[8] A. Fujisawa, H. Iguchi, M. Sasao, Y. Hamada, and J. Fujita, Rev. Sci. Instrum. **63**, 3694 (1992).
[9] T. Ido *et al.*, Rev. Sci. Instrum. **77**, 10F523 (2006).
[10] K. Ishii, M. Kotoku, T. Segawa, I. Katanuma, A. Mase, and S. Miyoshi, Rev. Sci. Instrum. **60**, 3270 (1989).
[11] D. W. Ross *et al.*, Rev. Sci. Instrum. **63**, 2232 (1992).
[12] J. W. Heard, T. P. Crowley, D. W. Ross, P. M. Schoch, R. L. Hickok, and B. Z. Zhang, Rev. Sci. Instrum. **64**, 1001 (1993).
[13] A. Fujisawa, H. Iguchi, S. Lee, and Y. Hamada, Rev. Sci. Instrum. **68**, 3393 (1997).
[14] H. Nakano, A. Fujisawa, A. Shimizu, S. Ohshima, T. Minami, Y. Yashimura, S. Okamura, and K. Matsuoka, Rev. Sci. Instrum. **75**, 3505 (2004).
[15] A. Fujisawa, A. Ouroua, J. W. Heard, T. P. Crowley, P. M. Schoch, K. A. Conner, R. L. Hickok, and A. J. Wootton, Nucl. Fusion **36**, 375 (1996).
[16] K. Matsuoka *et al.*, in Proceedings of the 12th International Conference on Plasma Physics and Controlled Nuclear Fusion Research, Nice, 1988 (International Atomic Energy Agency, Vienna, 1989), Vol. 2, p. 411.
[17] W. Lotz, Astrophys. J. **14**, 207 (1967).